



HAL
open science

The effect of the environment on the H I scaling relations

A. Boselli, S. Heinis, L. Cortese, B. Catinella, Samuel Boissier

► **To cite this version:**

A. Boselli, S. Heinis, L. Cortese, B. Catinella, Samuel Boissier. The effect of the environment on the H I scaling relations. *Monthly Notices of the Royal Astronomical Society*, 2011, 415 (2), pp.1797–1806. 10.1111/j.1365-2966.2011.18822.x . hal-01438873

HAL Id: hal-01438873

<https://hal.science/hal-01438873>

Submitted on 18 Dec 2021

HAL is a multi-disciplinary open access archive for the deposit and dissemination of scientific research documents, whether they are published or not. The documents may come from teaching and research institutions in France or abroad, or from public or private research centers.

L'archive ouverte pluridisciplinaire **HAL**, est destinée au dépôt et à la diffusion de documents scientifiques de niveau recherche, publiés ou non, émanant des établissements d'enseignement et de recherche français ou étrangers, des laboratoires publics ou privés.



Distributed under a Creative Commons Attribution 4.0 International License

The effect of the environment on the H I scaling relations

L. Cortese,¹* B. Catinella,² S. Boissier,³ A. Boselli³ and S. Heinis³

¹European Southern Observatory, Karl-Schwarzschild Str. 2, 85748 Garching bei Muenchen, Germany

²Max-Planck Institut für Astrophysik, D-85741 Garching bei München, Germany

³Laboratoire d'Astrophysique de Marseille, UMR6110 CNRS, 38 rue F. Joliot-Curie, 13388 Marseille, France

Accepted 2011 March 29. Received 2011 March 28; in original form 2011 March 9

ABSTRACT

We use a volume-, magnitude-limited sample of nearby galaxies to investigate the effect of the environment on the H I scaling relations. We confirm that the H I-to-stellar mass ratio anticorrelates with stellar mass, stellar mass surface density and $\text{NUV} - r$ colour across the whole range of parameters covered by our sample ($10^9 \lesssim M_* \lesssim 10^{11} M_\odot$, $7.5 \lesssim \mu_* \lesssim 9.5 M_\odot \text{ kpc}^{-2}$, $2 \lesssim \text{NUV} - r \lesssim 6 \text{ mag}$). These scaling relations are also followed by galaxies in the Virgo cluster, although they are significantly offset towards lower gas content. Interestingly, the difference between field and cluster galaxies gradually decreases moving towards massive, bulge-dominated systems. By comparing our data with the predictions of chemospectrophotometric models of galaxy evolution, we show that starvation alone cannot explain the low gas content of Virgo spirals and that only ram-pressure stripping is able to reproduce our findings. Finally, motivated by previous studies, we investigate the use of a plane obtained from the relations between the H I-to-stellar mass ratio, stellar mass surface density and $\text{NUV} - r$ colour as a proxy for the H I deficiency parameter. We show that the distance from the ‘H I gas fraction plane’ can be used as an alternative estimate for the H I deficiency, but only if carefully calibrated on pre-defined samples of ‘unperturbed’ systems.

Key words: galaxies: clusters: individual: Virgo – galaxies: evolution – galaxies: fundamental parameters – radio lines: galaxies – ultraviolet: galaxies.

1 INTRODUCTION

Understanding the role played by the cold gas component in galaxy evolution is one of the main challenges for extragalactic studies. The cold atomic hydrogen (H I) is the reservoir out of which all stars are eventually formed. Therefore, a detailed knowledge of its relation to other galaxy properties is of primary importance in order to build a coherent picture of galaxy evolution.

Although the direct detection of H I emission from individual galaxies is still technically limited to the nearby universe (e.g. Verheijen et al. 2007; Catinella et al. 2008), in the last decades several studies have highlighted how the H I content (usually estimated as the H I mass-to-luminosity ratio) varies with morphology, luminosity, size and star formation activity (e.g. Roberts 1963; Haynes & Giovanelli 1984; Roberts & Haynes 1994; Gavazzi, Pierini & Boselli 1996; McGaugh & de Blok 1997; Boselli et al. 2001; Kannappan 2004). Particularly powerful appears to be the use of 21-cm data to investigate environmental effects. Several studies

have shown that H I-deficient¹ galaxies are mainly/only present in very high density environments (Giovanelli & Haynes 1985; Cayatte et al. 1990; Solanes et al. 2001; Boselli & Gavazzi 2009), providing strong constraints on the possible environmental mechanisms responsible for the quenching of the star formation in clusters of galaxies (see Boselli & Gavazzi 2006, and references therein).

Unfortunately, a great part of what we know about H I in galaxies has been achieved by studying relatively small samples, with not always well-defined selection criteria, often focused on specific morphological classes (e.g. only late-type galaxies) and with small overlap with multiwavelength surveys, necessary to investigate how the cold gas correlates with other baryonic components. Moreover, it is very difficult for simulations to provide accurate estimates for important observables like the H I deficiency parameter (since it is based on a detailed morphological classification), limiting the comparison between observations and theory. In other words, H I astronomy is in a situation similar to the one of optical and

¹The H I deficiency ($\text{Def}_{\text{H I}}$) is defined as the difference, in logarithmic units, between the expected H I mass for an isolated galaxy with the same morphological type and optical diameter of the target and the observed value (Haynes & Giovanelli 1984).

*E-mail: lcortese@eso.org

ultraviolet astronomy before the Sloan Digital Sky Survey (SDSS) and the *Galaxy Evolution Explorer* (*GALEX*) mission. The main scaling relations (e.g. colour–magnitude, size–luminosity, etc.) were already known, but a detailed quantification of their properties, crucial for a comparison with models, was still missing.

Luckily, the situation is rapidly changing for 21-cm studies. The advent of large H I surveys, such as the Arecibo Legacy Fast ALFA (ALFALFA) survey (Giovanelli et al. 2005), which eventually will provide H I masses for a few tens of thousands of galaxies over areas of sky with large multiwavelength coverage, is gradually allowing detailed statistical analysis of H I properties in the local universe. Very promising results in this direction have been recently obtained by the *GALEX* Arecibo SDSS Survey (GASS; Catinella et al. 2010), a targeted survey of a volume-limited sample of ~ 1000 massive galaxies ($M_* > 10^{10} M_\odot$). Catinella et al. (2010) used the first GASS data release to quantify the main scaling relations linking the H I-to-stellar mass ratio to stellar mass, stellar mass surface density and colour. They also suggested the existence of a ‘gas fraction plane’ linking H I gas fraction² to stellar mass surface density and NUV – r colour and proposed to use this plane to isolate interesting outliers that might be in the process of accreting or losing a significant fraction of their gas content. In this context, the plane might be considered as an alternative way to define H I deficiency when accurate morphological classification is not available. However, this hypothesis has never been tested for a sample for which both H I deficiency and the H I gas fraction plane can be estimated independently.

In this paper, we use a volume-, magnitude-limited sample of ~ 300 galaxies to extend the study of the H I scaling relations to a larger dynamical range in stellar mass and stellar mass surface density and to different environments (i.e. from isolated systems to the centre of the Virgo cluster). Our main goals are (i) to accurately quantify the effect of the cluster environment on the H I scaling relations, (ii) to investigate the validity of the H I plane as a proxy for H I deficiency and (iii) to highlight the power of H I scaling relations to constrain models of galaxy formation and evolution.

2 THE SAMPLE

The analysis presented in this paper is based on the Herschel Reference Survey (HRS; Boselli et al. 2010). Briefly, this consists of a volume-limited sample (i.e. $15 \leq d \leq 25$ Mpc) including late-type galaxies (Sa and later) with Two Micron All-Sky Survey (Skrutskie et al. 2006) K -band magnitude $K_{\text{Stot}} \leq 12$ mag and early-type galaxies (S0a and earlier) with $K_{\text{Stot}} \leq 8.7$ mag. Additional selection criteria are high galactic latitude ($b > +55^\circ$) and low Galactic extinction ($A_B < 0.2$ mag; Schlegel, Finkbeiner & Davis 1998), to minimize Galactic cirrus contamination. The total sample consists of 322 galaxies (260 late- and 62 early-type galaxies).³ As extensively discussed in Boselli et al. (2010), this sample is not only representative of the local universe but, spanning different density regimes (i.e. from isolated systems to the centre of the Virgo cluster), it is also ideal for environmental studies (see also Cortese & Hughes 2009).

Atomic hydrogen masses have been estimated from H I 21-cm line-emission data (mainly single dish), available from the litera-

ture [e.g. Gavazzi et al. 2003; Springob, Haynes & Giovanelli 2005; Giovanelli et al. 2007; Kent et al. 2008 and the NASA/IPAC Extragalactic Database (NED)]. In total, 305 out of 322 galaxies in the HRS (~ 95 per cent) have been observed at 21 cm, with 265 detections and 40 non-detections. H I masses have been computed via

$$\frac{M(\text{H I})}{M_\odot} = 2.356 \times 10^5 \frac{S_{\text{H I}}}{\text{Jy km s}^{-1}} \left(\frac{d}{\text{Mpc}} \right)^2, \quad (1)$$

where $S_{\text{H I}}$ is the integrated H I line flux density and d is the distance. As discussed in Boselli et al. (2010), we fixed the distances for galaxies belonging to the Virgo cluster (i.e. 23 Mpc for the Virgo B cloud and 17 Mpc for all the other clouds; Gavazzi et al. 1999), while for the rest of the sample distances have been estimated from their recessional velocities assuming a Hubble constant $H_0 = 70 \text{ km s}^{-1} \text{ Mpc}^{-1}$. In case of non-detections, upper limits have been determined assuming a 5σ signal with 300 km s^{-1} velocity width. We estimate the H I deficiency parameter ($\text{Def}_{\text{H I}}$) following Haynes & Giovanelli (1984). The expected H I mass for each galaxy is determined via

$$\log(M(\text{H I})_{\text{exp}}) = a_{\text{H I}} + b_{\text{H I}} \times \log \left(\frac{hD_{25}}{\text{kpc}} \right) - 2 \log(h), \quad (2)$$

where $h = H_0/100 \text{ km s}^{-1} \text{ Mpc}^{-1}$, D_{25} is the optical isophotal diameter measured at 25 mag arcsec² in B band and $a_{\text{H I}}$ and $b_{\text{H I}}$ are two coefficients that vary with morphological type. These coefficients have been calculated for the following types (see also table 3 in Boselli & Gavazzi 2009): S0a and earlier (Haynes & Giovanelli 1984), Sa-Sab, Sb, Sbc, Sc (Solanes, Giovanelli & Haynes 1996) and Scd to Irr (Boselli & Gavazzi 2009). Morphological classifications for our sample are taken from the Virgo Cluster Catalogue (Binggeli, Sandage & Tammann 1985), NED and Boselli et al. (2010). The H I deficiency is then

$$\text{Def}_{\text{H I}} = \log(M(\text{H I})_{\text{exp}}) - \log(M(\text{H I})). \quad (3)$$

We note that the estimate of the expected H I mass for early-type galaxies is extremely uncertain. As we will show later, this uncertainty can significantly affect the quantification of the H I scaling relations. In the following, we will consider as ‘H I-deficient’ galaxies those objects with $\text{Def}_{\text{H I}} \geq 0.5$ (i.e. galaxies with 70 per cent less hydrogen than isolated systems with the same diameter and morphological type). The average H I deficiency of galaxies with $\text{Def}_{\text{H I}} < 0.5$ is $\text{Def}_{\text{H I}} = 0.06 \pm 0.28$, consistent with the typical uncertainty in the estimate of $\text{Def}_{\text{H I}}$ for isolated field galaxies (Haynes & Giovanelli 1984; Solanes et al. 1996).

Ultraviolet and optical broad-band photometry have been obtained from *GALEX* (Martin et al. 2005) and SDSS Data Release 7 (DR7) (Abazajian et al. 2009) data bases, respectively. *GALEX* near-ultraviolet (NUV; $\lambda = 2316 \text{ \AA}$; $\Delta\lambda = 1069 \text{ \AA}$) images have been mainly obtained as part of two on-going *GALEX* Guest Investigator programmes (GI06-12, PI L. Cortese and GI06-01, *GALEX* Ultraviolet Virgo Cluster Survey (GUViCS), Boselli et al. 2011). Additional frames have been obtained from the *GALEX* GR6 public release. All frames have been reduced using the current version of the *GALEX* pipeline (ops-v7). The *GALEX* NUV and SDSS g , r , i photometry for the HRS was determined as follows. The SDSS images were registered to the *GALEX* frames and convolved to the NUV resolution (5.3 arcsec, Morrissey et al. 2007). Isophotal ellipses were then fitted to each image, keeping fixed the centre, ellipticity and position angle (generally determined in the i band). Asymptotic magnitudes have been determined from the growth curve obtained following the technique described by Gil de

² In this paper we will refer to the $M(\text{H I})/M_*$ ratio as gas fraction.

³ HRS228/LCRS B123647.4–052325 has been removed from the original sample since the redshift reported in NED was not correct and the galaxy lies well beyond the limits of the HRS, $z \sim 0.04$.

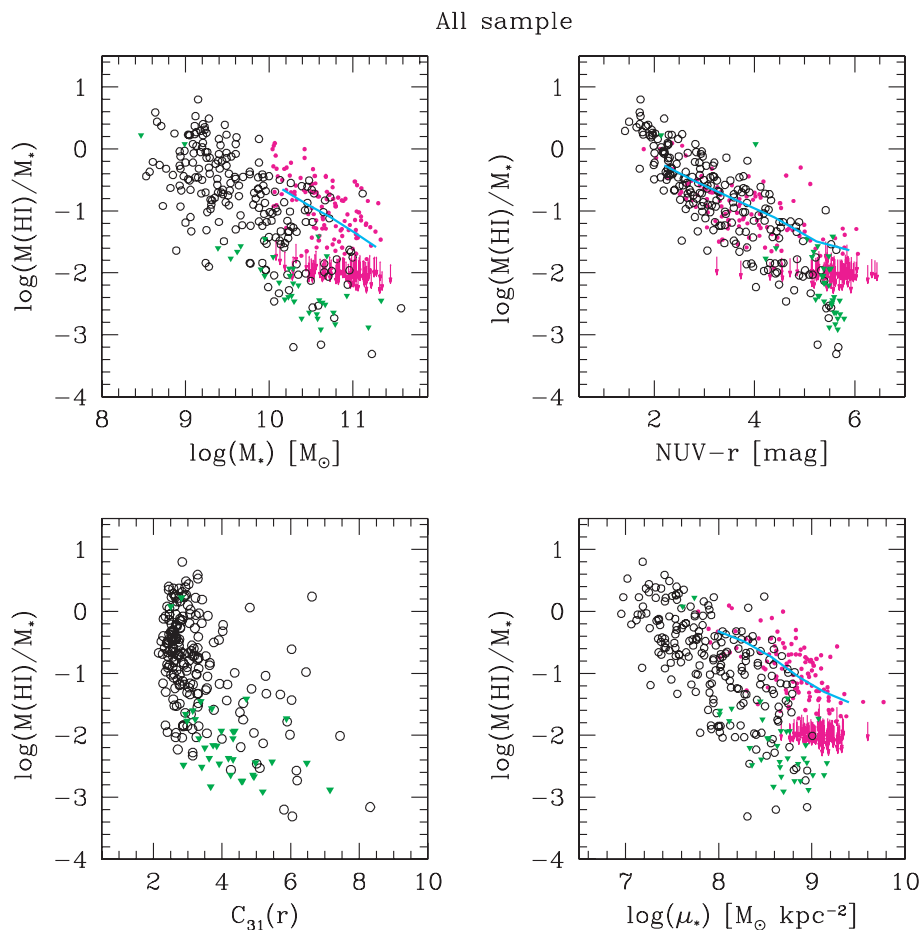


Figure 1. The H I mass fraction of the HRS plotted as a function of stellar mass, NUV $- r$ colour, concentration index and stellar mass surface density. Black circles and green triangles represent detections and non-detections, respectively. GASS DR1 detections and non-detections are indicated with magenta dots and arrows, respectively. The average scaling relations obtained from ALFALFA stacking of the GASS parent sample are indicated in cyan.

Paz et al. (2007) and corrected for Galactic extinction assuming a Cardelli, Clayton & Mathis (1989) extinction law with $A(V)/E(B - V) = 3.1$: i.e. $A(\lambda)/E(B - V) = 8.2$ (Wyder et al. 2007), 3.793, 2.751 and 2.086 for NUV, g , r and i , respectively. Stellar masses M_* are determined from i -band luminosities L_i using the $g - i$ colour-dependent stellar mass-to-light ratio relation from Zibetti, Charlot & Rix (2009), assuming a Chabrier (2003) initial mass function (IMF):

$$\log(M_*/L_i) = -0.963 + 1.032(g - i). \quad (4)$$

The final sample used for the following analysis includes those HRS galaxies for which H I, NUV and SDSS observations are currently available: 241 galaxies (~ 75 per cent of the whole HRS, namely 200 late- and 41 early-type galaxies).

3 THE H I SCALING RELATIONS OF THE HRS

In order to quantify how the H I gas fraction varies as a function of integrated galaxy properties, we plot in Fig. 1 the H I-to-stellar mass ratio as a function of stellar mass (upper left-hand panel), observed NUV $- r$ colour (upper right-hand panel), concentration index in r band [$C_{31}(r)$, defined as the ratio between the radii containing 75 and 25 per cent of the total r -band light] and stellar mass surface density [i.e. $M_*/(2\pi R_{50,i}^2)$, where $R_{50,i}$ is the radius containing 50 per cent of the total i -band light, i.e. the effective radius]. For comparison,

we also plot the data from the GASS DR1 (Catinella et al. 2010, magenta symbols) and from the stacking of ALFALFA observations for the GASS parent sample (Fabello et al. 2011, cyan line). Over the range of stellar masses covered by the HRS, the H I gas fraction strongly anticorrelates with M_* , NUV $- r$ [a proxy for specific star formation rate (SSFR)] and μ_* , while a very weak non-linear trend is observed with the concentration index. The tightest correlation is with the observed NUV $- r$ colour (Pearson correlation coefficient $r = -0.89$, dispersion along the y -axis $\sigma = 0.42$ dex),⁴ while the scatter gradually increases for the stellar surface density ($r = -0.74$, $\sigma = 0.61$ dex) and mass ($r = -0.72$, $\sigma = 0.63$ dex).

Our findings extend very nicely the results of the GASS survey (Catinella et al. 2010; Fabello et al. 2011) to lower stellar mass and surface densities, highlighting how the SFR, stellar mass and galaxy structure are tightly linked to the H I content of the local galaxy population. However, it is important to note that the scaling relations for the HRS are slightly offset towards lower gas fractions when compared to the results of the GASS survey. This difference is easily understood when we consider that, by construction, nearly half of the galaxies in the HRS belong to the Virgo cluster and, as a whole, this sample might be biased towards gas-poor objects. To test this and to characterize the H I scaling relations in different

⁴ These parameters are obtained assuming the non-detections to their upper limits.

environments, we have divided our sample in three different subsets: (i) galaxies with $\text{Def}_{\text{HI}} < 0.5$ (i.e. H I normal, 135 galaxies), (ii) galaxies outside the Virgo cluster (110 galaxies) and (iii) galaxies belonging to one of the Virgo cluster clouds (Virgo A, B, N, E and S as defined by Gavazzi et al. 1999, 131 galaxies). We note that, while (ii) and (iii) are complementary by construction, (i) may include both Virgo and field galaxies. The scaling relations for the three samples are plotted in Fig. 2. As expected, although for all samples the H I gas fraction decreases with stellar mass, colour and stellar mass surface density, galaxies in different environments

show significantly different H I content. Virgo galaxies have, on average, a lower H I-to-stellar mass ratio than H I-normal galaxies across the whole range of stellar masses and stellar mass surface densities covered by the HRS. In fact, the dispersion in the two scaling relations drops from ~ 0.62 dex for the whole sample to ~ 0.37 dex for H I-normal galaxies only.

In order to quantify the difference between cluster and field, in Fig. 3 we show the average trends [i.e. $\langle \log(M(\text{HI})/M_*) \rangle$] for each subsample. The averages are measured by assuming the non-detections to their upper limit and by correcting for the fact that we

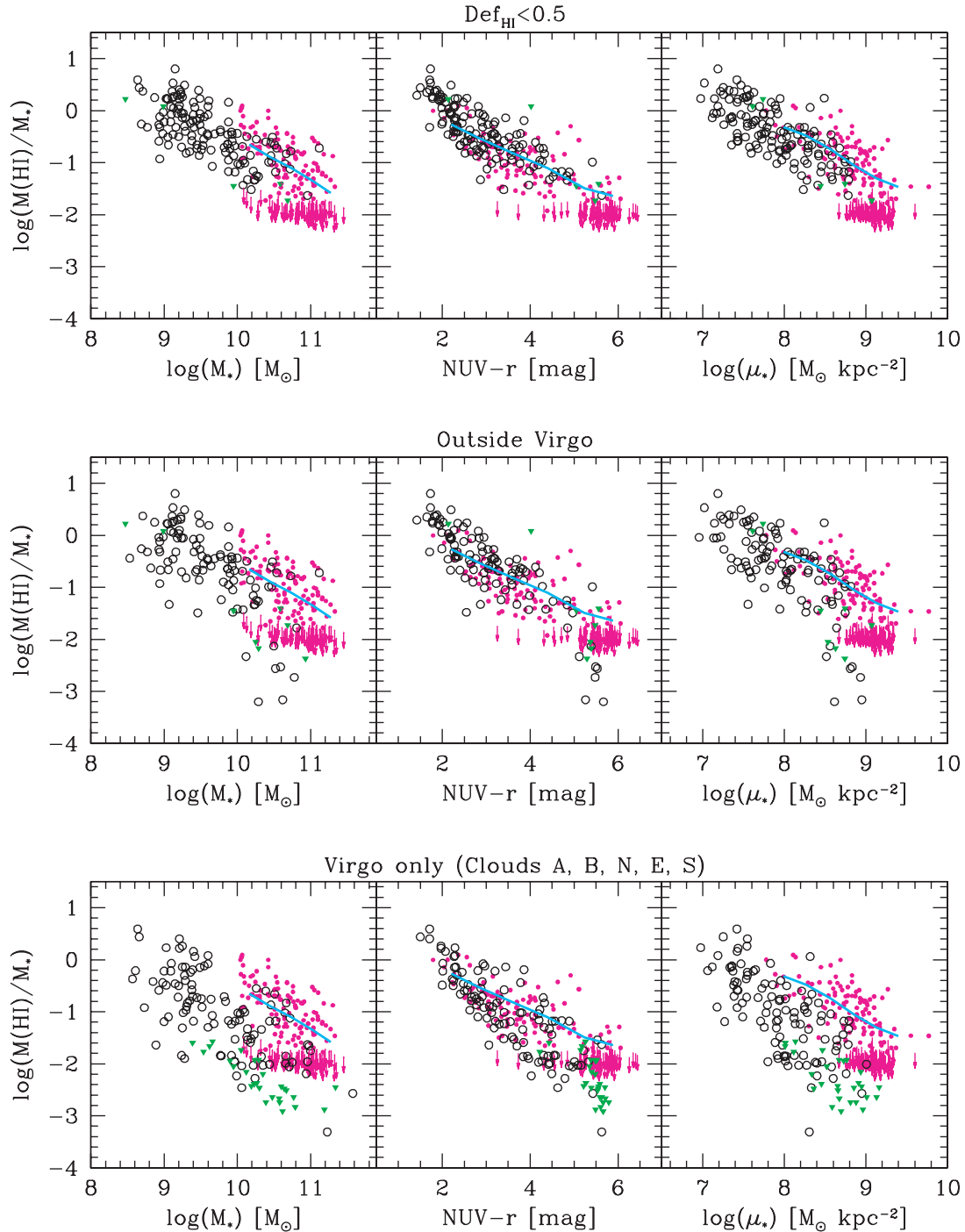


Figure 2. The H I mass fraction as a function of stellar mass, $\text{NUV} - r$ colour and stellar mass surface density for H I-normal galaxies (upper panel), galaxies outside the Virgo cluster (middle panel) and galaxies belonging to one of the Virgo cluster clouds (bottom panel). Symbols are as in Fig. 1.

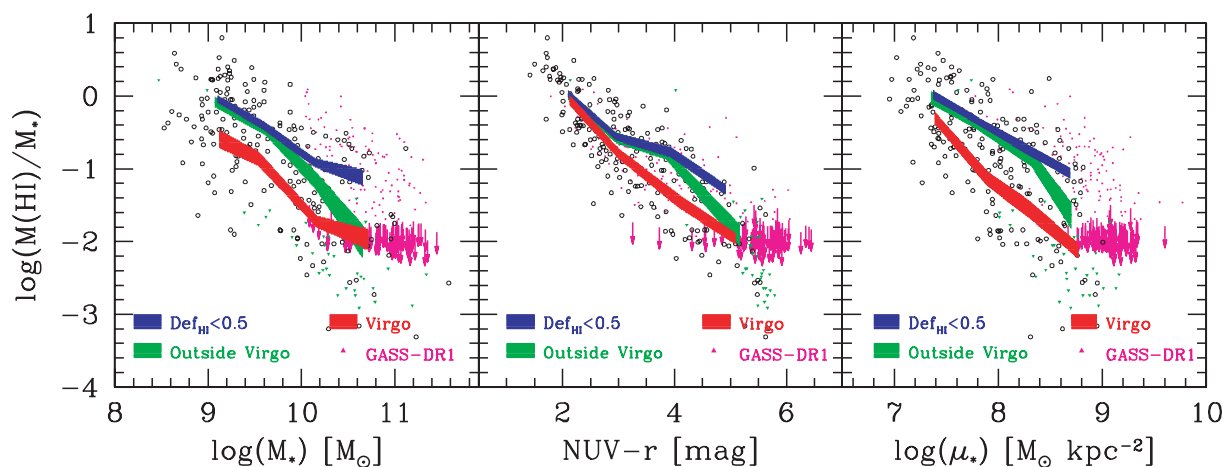


Figure 3. The average H I mass fraction [i.e. $\log(M(\text{HI})/M_*)$] scaling relations for different samples. H I-normal galaxies and systems belonging to or outside Virgo are indicated by blue, red and green lines, respectively. For comparison, GASS DR1 is shown in magenta.

do not have H I and ultraviolet data for all HRS galaxies. In practice, we weighted each galaxy by the completeness of the sample in its bin of K -band luminosity. The average scaling relations and the number of galaxies contributing to each bin are given in Table 1.

The difference between H I-normal and cluster galaxies varies by ~ 0.3 dex as a function of stellar mass (i.e. from ~ 0.55 to 0.85 dex), while it increases from ~ 0.25 to 1 dex when moving from disc- to bulge-dominated systems (i.e. from $\mu_* \sim 7.4$ to $8.7 M_\odot \text{ kpc}^{-2}$).⁵ Less strong is the environmental dependence of the gas fraction versus $\text{NUV} - r$ relation. Blue-sequence galaxies ($\text{NUV} - r < 3.5$ mag) have the same H I gas fraction regardless of the environment, consistent with a scenario in which actively star-forming cluster galaxies have just started their infall into the cluster centre (Boselli & Gavazzi 2006; Cortese, Gavazzi & Boselli 2008b). On the contrary, red Virgo galaxies are significantly gas poorer than H I-normal systems. It is important to note that this difference might be, at least partially, due to an extinction effect. While a significant fraction of red cluster galaxies are likely to be really passive systems, field red objects should be more heavily affected by internal dust attenuation. Therefore, bins of observed $\text{NUV} - r$ colour might not directly correspond to bins of SSFR. We plan to investigate this issue in a future paper, where *Herschel* data will be used to properly correct for internal dust absorption.

Interestingly, we find some differences also when comparing H I-normal galaxies to objects outside the Virgo clusters. Since H I-deficient galaxies are mainly/only found in clusters of galaxies (Haynes & Giovanelli 1984; Cortese et al. 2008a; Boselli & Gavazzi 2009), it is common practice to assume that galaxies in the field, in pairs and loose groups, are not H I-deficient (and vice versa). Our analysis shows that a one-to-one correlation between H I-normal galaxies and systems in low-/intermediate-density environments apparently breaks at high stellar masses ($M_* > 10^{10.4} M_\odot$), stellar mass surface densities ($\mu_* > 8.5 M_\odot \text{ kpc}^{-2}$) and red colours ($\text{NUV} - r > 4.5$ mag), where we find H I-deficient galaxies also outside the cluster environment. It is important to note that a significant fraction of these gas-poor galaxies [i.e. five out of seven

and six out of ten for the $\log(M(\text{HI})/M_*)$ versus $\log(M_*)$ and $\log(M(\text{HI})/M_*)$ versus $\log(\mu_*)$ relations, respectively] are early-type systems (S0a or earlier) for which the H I deficiency calibration is notoriously uncertain. Whether the typical red, massive, bulge-dominated galaxy contains a significant cold gas reservoir or not is still matter of debate. These ranges of stellar masses, colour and stellar surface densities have not been adequately sampled by previous H I investigations and it is not completely surprising that we find a difference between H I-normal and field galaxies.

Whatever the origin of the difference between H I-normal and ‘field’ galaxies, the break observed in the H I scaling relations for galaxies outside the Virgo cluster is very similar to the transition observed in the colour–stellar mass and colour–stellar mass surface density diagrams (e.g. Kauffmann et al. 2003). Bothwell, Kennicutt & Lee (2009) and Catinella et al. (2010) already reported the presence of a transition in the H I gas fraction versus stellar mass and stellar mass surface density relations, respectively (see also Kannappan 2004). Our analysis confirms both results at once independently, suggesting that the typical transitions observed in the colour–mass diagram might be related to the transition in H I gas fraction shown in Figs 2 and 3. Unfortunately, above the transition our statistics becomes too small and we will have to wait for larger H I surveys to characterize more in detail this break in the H I scaling relations.

Finally, it is important to point out that, above the transition in stellar mass/surface density, the difference in H I gas fraction between cluster and field galaxies tends to disappear. This provides an indirect support to a scenario in which environmental effects are today mainly active on the population of low-/intermediate-mass disc galaxies, while the properties of high-mass/bulge-dominated systems are less affected by the local density.

4 COMPARISON WITH MODELS

The results presented in Section 3 have shown that, at fixed stellar mass and surface densities, cluster galaxies have significantly lower H I content than galaxies in low-density environments. On one side, these results confirm that H I-deficient galaxies are mainly present in high-density environments (Haynes & Giovanelli 1984). On the other, they nicely complement previous analysis showing that cluster galaxies have in general a lower SFR than their field counterpart (Gavazzi et al. 2002; Gómez et al. 2003; Boselli & Gavazzi 2006), suggesting that the gas loss is behind the quenching

⁵ We remind the reader that, by construction, the HRS does not include intermediate-, low-mass early-type galaxies, typically found in high-density environments (Cortese & Hughes 2009; Hughes & Cortese 2009). Thus, for low stellar masses, low stellar mass surface densities and red colours, we might be underestimating the difference between cluster and field galaxies.

Table 1. The average scaling relations for the three samples discussed in Section 3.

x	$\langle x \rangle$	$\langle \log(M(\text{H I})/M_*) \rangle^a$	N_{gal}
H I normal ($\text{Def}_{\text{H I}} < 0.5$)			
$\log(M_*)$	9.10	-0.04 ± 0.05	46
	9.59	-0.40 ± 0.06	44
	10.15	-0.92 ± 0.06	31
	10.66	-1.12 ± 0.11	10
NUV $- r$	2.10	$+0.03 \pm 0.05$	52
	2.96	-0.56 ± 0.05	46
	3.93	-0.77 ± 0.07	25
	4.92	-1.29 ± 0.07	9
$\log(\mu_*)$	7.37	$+0.02 \pm 0.06$	36
	7.80	-0.34 ± 0.05	48
	8.30	-0.75 ± 0.07	32
	8.69	-1.06 ± 0.07	16
Outside Virgo			
$\log(M_*)$	9.07	-0.08 ± 0.07	36
	9.62	-0.47 ± 0.07	31
	10.14	-1.14 ± 0.12	29
	10.66	-2.00 ± 0.23	11
NUV $- r$	2.10	$+0.01 \pm 0.06$	36
	2.95	-0.57 ± 0.07	34
	3.85	-0.79 ± 0.08	20
	5.17	-1.92 ± 0.15	16
$\log(\mu_*)$	7.35	-0.02 ± 0.09	21
	7.78	-0.37 ± 0.07	40
	8.32	-0.86 ± 0.11	25
	8.70	-1.64 ± 0.18	21
Virgo			
$\log(M_*)$	9.12	-0.59 ± 0.12	26
	9.54	-0.86 ± 0.10	33
	10.17	-1.73 ± 0.08	43
	10.72	-1.97 ± 0.14	22
NUV $- r$	2.13	-0.06 ± 0.07	21
	3.00	-0.79 ± 0.07	34
	4.09	-1.45 ± 0.09	32
	5.09	-1.96 ± 0.08	28
$\log(\mu_*)$	7.39	-0.30 ± 0.08	29
	7.89	-1.13 ± 0.10	35
	8.30	-1.56 ± 0.12	34
	8.77	-2.13 ± 0.10	30

^aWe note that these are averages of $\log(M(\text{H I})/M_*)$ and not $M(\text{H I})/M_*$ (as in Catinella et al. 2010). We preferred this approach because the distribution of H I gas fraction is closer to a lognormal than to a Gaussian.

of the star formation activity (Gavazzi et al. 2006; Cortese & Hughes 2009). Although this scenario is commonly accepted, there is still debate about the environmental mechanism(s) responsible for such differences between low- and high-density environments (e.g. Weinmann, van den Bosch & Pasquali 2011). In particular, it is not clear whether the H I is stripped directly from the disc via a strong interaction with the dense intracluster medium (i.e. ram-pressure stripping; Gunn & Gott 1972) or if the gas is just removed from the extended gaseous halo surrounding the galaxy, preventing further infall (i.e. starvation; Larson, Tinsley & Caldwell 1980). Boselli et al. (2008) have recently used multizone chemical and spectrophotometric models to constrain the evolutionary history of

dwarf galaxies in the Virgo cluster and to discriminate between the ram-pressure and starvation scenarios. They showed that the properties of most of the dwarfs dominating the faint end of the Virgo luminosity function are consistent with a scenario in which these galaxies were initially star-forming systems, accreted by the cluster and stripped of their gas by one or more ram-pressure stripping events.

Here, we use the same approach adopted by Boselli et al. (2008) to carry out a similar test for intermediate and massive galaxies in the Virgo cluster. The details of the models here adopted can be found in Boselli et al. (2008, appendix B). Briefly, the evolution of galaxies is traced using the multizone chemical and spectrophotometric model of Boissier & Prantzos (2000), updated with an empirically determined star formation law (Boissier et al. 2003) relating the SFR to the total gas surface densities. Following Boselli et al. (2008), we modified the original models to simulate the effects induced by the interaction with the cluster environment. In the starvation scenario, we simply stopped the infall of pristine gas in the model. We investigate interactions that started between 0 and 9.5 Gyr ago. The ram-pressure stripping event is simulated by assuming a gas-loss rate inversely proportional to the potential of the galaxy, with an efficiency depending on the density of the intracluster medium (taken from Vollmer et al. 2001). We assume two different values for the peak efficiency of ram-pressure stripping ($\epsilon_0 = 0.4$ and $1.2 M_{\odot} \text{ kpc}^{-2} \text{ yr}^{-1}$) and an age of the interaction between 0 and 5 Gyr ago. Models have been generated assuming a spin parameter $\lambda = 0.05$ and four different rotational velocities ($V_C = 100, 130, 170, 220 \text{ km s}^{-1}$), in order to cover the whole range of stellar masses spanned by the HRS. In order to convert the output of the model into the observables considered here, we proceeded as follows. Stellar masses have been converted from a Kroupa, Tout & Gilmore (1993), used in the model, to a Chabrier (2003) IMF by adding 0.06 dex (Bell et al. 2003; Gallazzi et al. 2008). Stellar mass surface densities have been determined using the effective radius in i band, as done for our data. H I masses are obtained from the total gas mass by removing the contribution of helium and heavy elements (i.e. a factor of 1.36) and assuming a molecular-to-atomic hydrogen gas ratio of 0.38, independent of stellar mass (Saintonge et al. 2011). NUV $- r$ colours have been ‘reddened’ by assuming an average internal extinction $A(\text{NUV}) = 1$ mag. This value is quite arbitrary and will likely depend on the evolutionary history of each galaxy. However, this assumption does not affect our main conclusions. Finally, we note that the goal of this exercise is to establish which scenario is more consistent with our data, not to determine the best model fitting our observations. There are many free parameters and assumptions in the modelling that could be tweaked in order to better match our observations, but looking for an exact fit does not seem meaningful given the simple description adopted here.

In Fig. 4 (top panels) we compare the predictions of the starvation model with our data. The filled circles indicate the predictions for the unperturbed models. The models seem to fairly reproduce the NUV $- r$ and μ_* versus gas fraction scaling relations observed for H I-normal and field galaxies. However, a significant difference between data and models is observed in the $M(\text{H I})/M_*$ versus M_* relation: for very high stellar masses (rotation velocities), the unperturbed model predicts gas fractions ~ 0.5 dex higher than the average observed value. This likely reflects the fact that the model is only valid for disc galaxies and does not include any bulge component. It is thus not surprising that at high masses, where the fraction of bulge-dominated galaxies increases, the predictions we obtain are not representative of the whole population (although still well

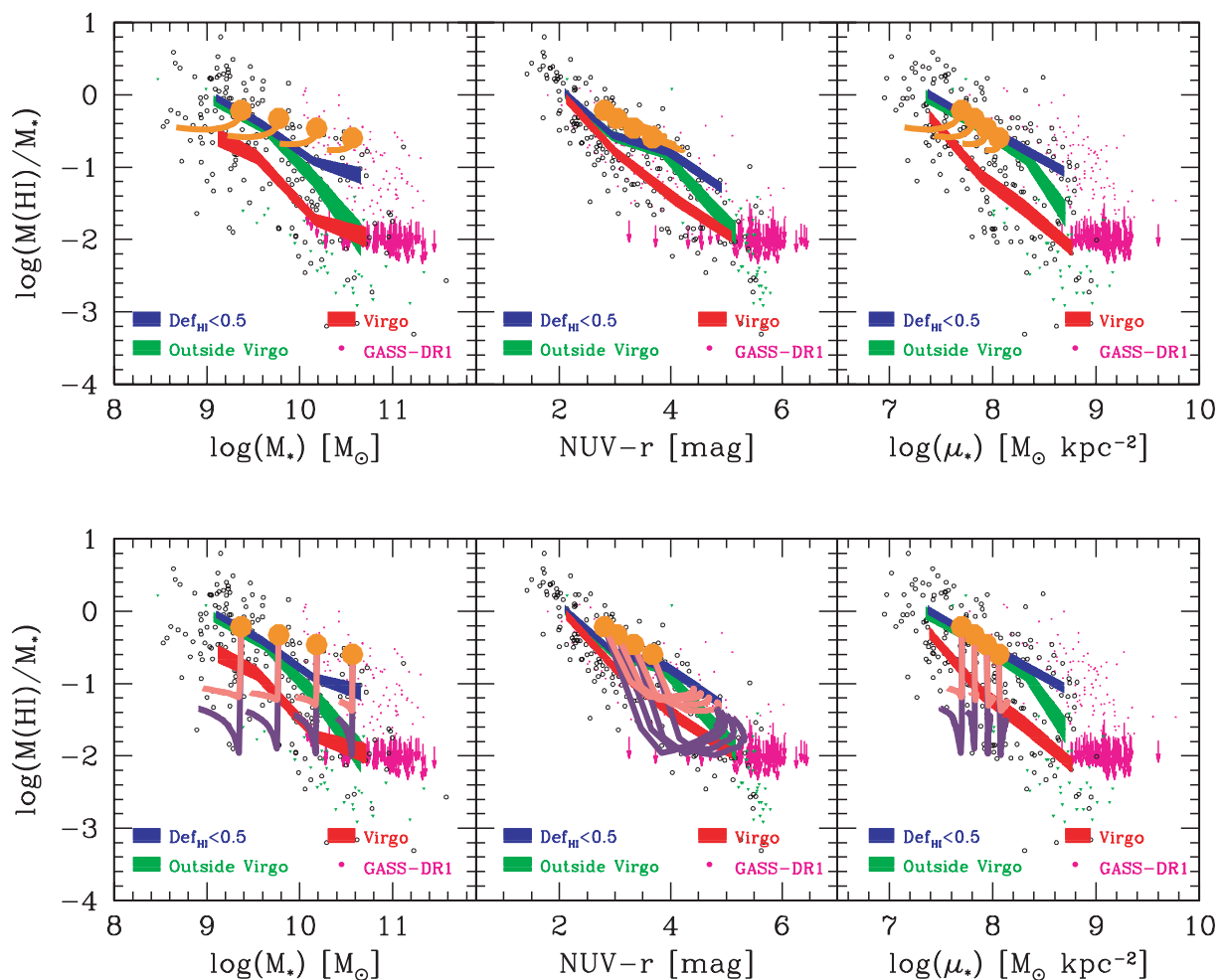


Figure 4. Model predictions for a starvation (upper panels) and ram-pressure stripping (lower panels) event. In case of starvation we considered ages between 0 and 9.5 Gyr, while for ram pressure we restricted our analysis to events occurred between 0 and 5 Gyr ago. In both sets of panels, the unperturbed model is indicated by the filled circles. In the bottom panel, the two lines indicate models for different ram-pressure efficiencies: $\epsilon_0 = 0.4$ (light curve) and $1.2 M_{\odot} \text{ kpc}^{-2} \text{ yr}^{-1}$ (dark curve). Data are as in Fig. 3. We note that these are not evolutionary tracks, but illustrate where a galaxy would lie today depending on the age of the interaction.

within the range of gas fractions covered by the observations). This is also confirmed by the fact that the model covers just the range of stellar mass surface densities typical of disc galaxies.

By comparing the predictions of the starvation model with our data, it clearly emerges that starvation is only able to mildly affect the H I content, even for very old events. The H I gas fraction decreases by only $\lesssim 0.25$ dex, i.e. within the intrinsic dispersion of the scaling relation for H I-normal galaxies. This decrease is even lower in the $M(\text{H I})/M_*$ versus $\text{NUV} - r$ plot, where galaxies affected by starvation lie on the main relation observed for unperturbed galaxies. It is thus impossible to reproduce the difference between cluster and field galaxies by just stopping the infall of gas on to the disc.

Much more promising are the results obtained for the ram-pressure stripping model (Fig. 4, bottom panels). For all the three scaling relations observed here, ram-pressure stripping is able to fairly reproduce the difference observed between cluster and field galaxies. A maximum efficiency of $0.4 M_{\odot} \text{ kpc}^{-2} \text{ yr}^{-1}$ (light curve) is sufficient to reproduce the average decrease in H I content for Virgo galaxies, while a higher efficiency ($1.2 M_{\odot} \text{ kpc}^{-2} \text{ yr}^{-1}$, dark curve) is necessary to explain some of the most H I-deficient systems in our sample. As expected, the $M(\text{H I})/M_*$ versus $\text{NUV} - r$ is the relation least affected by the environment. Once the gas is

removed, the star formation is quickly reduced and the perturbed galaxy will not shift considerably from the main relation. In conclusion, only the direct removal of gas from the star-forming disc is able to reproduce the significant difference between the H I scaling relations of cluster and field galaxies.

5 THE H I GAS FRACTION PLANE AND THE H I DEFICIENCY PARAMETER

In the previous sections we have confirmed the existence of a tight relation between H I gas fraction, stellar mass surface density and $\text{NUV} - r$ colour. Recent works have used these three quantities to define a ‘gas fraction plane’ to be used in order to determine gas fractions for large samples lacking H I observations (Zhang et al. 2009, using optical colours) and to isolate galaxies in the process of accreting or losing a significant amount of gas (Catinella et al. 2010). As discussed by Zhang et al. (2009), the existence of this plane can be seen as a direct consequence of the Kennicutt–Schmidt relation. In order to test how good the gas fraction plane is as a proxy for H I deficiency, we decided to compare the two approaches for our sample. We thus fitted a plane to the two-dimensional relation between H I mass fraction, stellar mass surface density and $\text{NUV} - r$

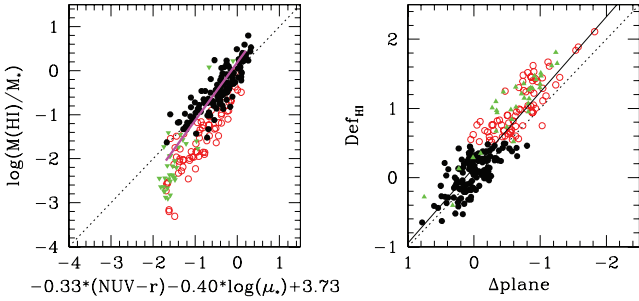


Figure 5. Left-hand panel: the H I gas fraction plane for H I-normal ($\text{Def}_{\text{HI}} < 0.5$) HRS galaxies. The H I gas fraction plane obtained for GASS galaxies is indicated by the magenta line. Right-hand panel: the correlation between H I deficiency and distance (along the y-axis) from the plane. The solid line indicates the best linear fit to the H I detections. In both panels, H I-normal, H I-deficient galaxies and non-detections are indicated with black filled circles, red empty circles and green triangles, respectively, and the dotted line shows the 1:1 anticorrelation.

colour for H I-normal galaxies only ($\text{Def}_{\text{HI}} < 0.5$), following the methodology outlined in Bernardi et al. (2003), i.e. by minimizing the residuals from the plane. The best fit to the plane is

$$\log\left(\frac{M(\text{HI})}{M_*}\right) = -0.33(\text{NUV} - r) - 0.40 \log(\mu_*) + 3.73 \quad (5)$$

and has a dispersion of only ~ 0.27 dex, comparable to the typical uncertainty in the H I deficiency parameter. The plane so obtained is illustrated in Fig. 5 (left-hand panel) and is fairly consistent with the one determined for the GASS sample by Catinella et al. (2010, magenta line). Given the different data sets and selection criteria adopted by the two surveys, this agreement is quite remarkable and indicates that both H I-normal HRS and GASS samples provide a fair representation of the H I properties of massive galaxies in the local universe. As expected, H I-deficient galaxies (empty circles) are significantly offset from the plane, having a lower H I content than what expected for their colour and stellar surface density. The distance from the plane along the y-axis [i.e. $\log(M_{\text{HI}}/M_*)_{\text{obs}} - \log(M_{\text{HI}}/M_*)_{\text{plane}}$] strongly anticorrelates with the H I deficiency (Fig. 5, right-hand panel). The best linear fit for the H I detections is

$$\text{Def}_{\text{HI}} = (-1.09 \pm 0.04) \times \Delta_{\text{plane}} + (0.14 \pm 0.02), \quad (6)$$

with ~ 0.25 dex dispersion. Again, the scatter is similar to the intrinsic scatter in the definition of the H I deficiency, suggesting that the H I plane is a tool as good as the H I deficiency to isolate extremely H I-rich or H I-poor galaxies, in particular when accurate morphological classification is not available.

Although the results obtained here are very promising, we want to conclude this section with some notes of caution in the definition, and use, of the H I gas fraction plane. The definition of a plane for H I-normal galaxies is justified by the fact that, for this sample, we observe a linear correlation between $\log(M(\text{HI})/M_*)$ and both $\text{NUV} - r$ colour and $\log(\mu_*)$. As discussed in the previous section, these linear relations are not valid for typical ‘field’ galaxies across the whole range of parameter investigated here, but we find a break for massive, bulge-dominated, red galaxies. Therefore, when these objects are included, the concept of a plane is no longer justified. In order to show how important is the sample selection, we plot in Fig. 6 the plane obtained for galaxies outside the Virgo cluster and compare it with what previously obtained for H I-normal galaxies (solid line). The two planes are significantly different, in particular at low H I gas fractions where there is an offset up to a factor of ~ 4 in the estimate of the H I mass. Incidentally, this shows once more how

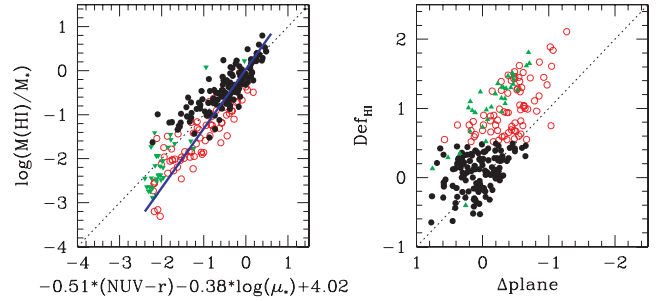


Figure 6. Left-hand panel: the H I gas fraction plane for HRS galaxies outside the Virgo cluster. The H I gas fraction plane obtained for H I-normal HRS galaxies (Fig. 5) is indicated by the solid line. Right-hand panel: the correlation between H I deficiency and distance (along the y-axis) from the plane. Symbols are as in Fig. 5.

‘field’ galaxies are not the same as ‘H I-normal’ systems. Moreover, this new plane is almost useless to isolate H I-deficient galaxies. H I-poor systems are no longer strong outliers and the relation between H I deficiency and distance from the plane is too scattered ($\sigma \sim 0.4$ dex) to be useful. We note that the good agreement between our plane for H I-normal galaxies and the one obtained using GASS detections is due to the fact that both data sets sample the stellar mass surface density regime below the break in H I gas fraction. Note that, if the GASS detection limit was much deeper than 1.5 per cent gas fraction (which roughly corresponds to the limit separating H I-normal and H I-deficient galaxies at high stellar masses, see Fig. 2), then this survey would include detections above the μ_* break, where the definition of a plane is no longer justified.

In conclusion, the H I gas fraction plane is a promising tool to estimate gas fractions and isolate outliers, but only if calibrated on well-defined samples of ‘normal’ unperturbed galaxies.

6 CONCLUSIONS

In this paper we have shown the relations between H I-to-stellar mass ratio, galaxy structure and colour for the HRS, a volume-, magnitude-limited sample of nearby galaxies. H I gas fractions anticorrelate with stellar mass, stellar mass surface density and $\text{NUV} - r$ colour, confirming previous results (e.g. Catinella et al. 2010). We show that these trends are observed in both low- and high-density environments, with the only difference that the scaling relations for cluster galaxies are shifted towards lower gas fractions. Thus, the cluster environment seems to have just a secondary (although important) role on galaxy evolution, with the efficiency of gas consumption and star formation mainly driven by the intrinsic ‘size’ (e.g. total mass) of the system (Gavazzi et al. 1996; Boselli et al. 2001; Kauffmann et al. 2003). Our findings nicely complement the scaling relations between SSFR and galaxy properties revealed by large optical and ultraviolet surveys (Blanton et al. 2005; Schiminovich et al. 2007). Naturally, because the H I is the fuel for star formation, it is likely that the link between SSFR and integrated properties is driven by the scaling relations presented here. This is also supported by the presence of a break in the $M(\text{HI})/M_*$ versus μ_* and $M(\text{HI})/M_*$ versus M_* relations, very close to the typical value characterizing the transition between the blue cloud and red sequence.

In order to shed light on the environmental mechanism responsible for the lower H I content of cluster galaxies, we compared our results with the predictions of the chemo-spectrophotometric model by Boissier & Prantzos (2000). We find that simply halting the infall

of pristine gas from the halo, mimicking the effect of starvation, is not sufficient to reproduce our observations. Only the stripping of gas directly from the star-forming disc (i.e. ram pressure) is able to match our data. This naturally explains why H I-deficient galaxies are mainly/only found in very high density environments, where ram-pressure stripping is efficient. However, it is important to note that our results do not imply that starvation is not playing any role on galaxy evolution. They just show that, if galaxies suffer starvation, their star formation activity and gas content can be changed, but the shape of the main H I scaling relations will not be significantly altered. We remind the reader that these results are only valid for disc galaxies. At high masses, where bulge-dominated systems dominate, not only our model cannot be used but also, most importantly, the difference between field and cluster starts to disappear, suggesting that the origin of the lower H I content of these objects cannot be only due to the cluster environment.

One of the interesting outcomes of our analysis is that, at high stellar masses, ‘field’ galaxies are not the same as ‘H I-normal’ objects. If confirmed, this clear difference might have important implications in our understanding of environmental effects in the local universe. In particular, one of the main issues for environmental studies is to reconcile the evidence that the effects of the environment start at densities typical of poor groups (Blanton & Moustakas 2009, and references therein) with the fact that H I-deficient objects are only observed in clusters of galaxies. Our analysis suggests that, from a statistical point of view, H I-deficient galaxies are clearly segregated in high-density environments only for $M_* \lesssim 10^{10} M_\odot$ and $\mu_* \lesssim 10^8 M_\odot \text{ kpc}^{-2}$ or, in other words, that intermediate-/low-mass gas-poor quiescent discs are only found in clusters of galaxies. Thus, the results obtained from H I data turn out to be fully consistent with what shown by optical studies: i.e. the intermediate-/low-mass part of the red sequence is only populated in clusters of galaxies (Baldry et al. 2006; Haines, Gargiulo & Merluzzi 2008; Gavazzi et al. 2010).

Finally, we have confirmed that the H I gas fraction plane defined by Catinella et al. (2010) can be used as an alternative to the H I deficiency parameter. However, we have also illustrated how important is the sample selection in the definition of the H I gas fraction plane and that, as for the H I deficiency, its use is mainly valid for galaxies below the threshold in μ_* .

Our results clearly highlight the importance of H I scaling relations for environmental studies and the necessity to extend this approach to larger samples and to a wider range of environments in order to understand in detail the role played by nurture in galaxy evolution.

ACKNOWLEDGMENTS

We thank the *GALEX* Time Allocation Committee for the time granted to the HRS and GUViCS projects.

GALEX is a NASA Small Explorer, launched in 2003 April. We gratefully acknowledge NASA’s support for construction, operation and science analysis for the *GALEX* mission, developed in cooperation with the Centre National d’Etudes Spatiales (CNES) of France and the Korean Ministry of Science and Technology.

This publication makes use of data products from Two Micron All Sky Survey, which is a joint project of the University of Massachusetts and the Infrared Processing and Analysis Center/California Institute of Technology, funded by the National Aeronautics and Space Administration and the National Science Foundation.

Funding for the SDSS and SDSS-II has been provided by the Alfred P. Sloan Foundation, the Participating Institutions, the National Science Foundation, the US Department of Energy, the National Aeronautics and Space Administration, the Japanese Monbukagakusho, the Max Planck Society and the Higher Education Funding Council for England. The SDSS website is <http://www.sdss.org/>.

The SDSS is managed by the Astrophysical Research Consortium for the Participating Institutions. The Participating Institutions are the American Museum of Natural History, Astrophysical Institute Potsdam, University of Basel, University of Cambridge, Case Western Reserve University, University of Chicago, Drexel University, Fermilab, the Institute for Advanced Study, the Japan Participation Group, Johns Hopkins University, the Joint Institute for Nuclear Astrophysics, the Kavli Institute for Particle Astrophysics and Cosmology, the Korean Scientist Group, the Chinese Academy of Sciences (LAMOST), Los Alamos National Laboratory, the Max-Planck-Institute for Astronomy (MPIA), the Max-Planck-Institute for Astrophysics (MPA), New Mexico State University, Ohio State University, University of Pittsburgh, University of Portsmouth, Princeton University, the United States Naval Observatory and the University of Washington.

We acknowledge the use of the NASA/IPAC Extragalactic Database (NED) which is operated by the Jet Propulsion Laboratory, California Institute of Technology, under contract with the National Aeronautics and Space Administration and of the GOLD-Mine data base.

REFERENCES

- Abazajian K. N. et al., 2009, *ApJS*, 182, 543
 Baldry I. K., Balogh M. L., Bower R. G., Glazebrook K., Nichol R. C., Bamford S. P., Budavari T., 2006, *MNRAS*, 373, 469
 Bell E. F., McIntosh D. H., Katz N., Weinberg M. D., 2003, *ApJS*, 149, 289
 Bernardi M. et al., 2003, *AJ*, 125, 1866
 Binggeli B., Sandage A., Tammann G. A., 1985, *AJ*, 90, 1681
 Blanton M. R., Moustakas J., 2009, *ARA&A*, 47, 159
 Blanton M. R., Eisenstein D., Hogg D. W., Schlegel D. J., Brinkmann J., 2005, *ApJ*, 629, 143
 Boissier S., Prantzos N., 2000, *MNRAS*, 312, 398
 Boissier S., Prantzos N., Boselli A., Gavazzi G., 2003, *MNRAS*, 346, 1215
 Boselli A., Gavazzi G., 2006, *PASP*, 118, 517
 Boselli A., Gavazzi G., 2009, *A&A*, 508, 201
 Boselli A., Gavazzi G., Donas J., Scodreggio M., 2001, *AJ*, 121, 753
 Boselli A., Boissier S., Cortese L., Gavazzi G., 2008, *ApJ*, 674, 742
 Boselli A. et al., 2010, *PASP*, 122, 261
 Boselli A. et al., 2011, *A&A*, 528, 107
 Bothwell M. S., Kennicutt R. C., Lee J. C., 2009, *MNRAS*, 400, 154
 Cardelli J. A., Clayton G. C., Mathis J. S., 1989, *ApJ*, 345, 245
 Catinella B., Haynes M. P., Giovanelli R., Gardner J. P., Connolly A. J., 2008, *ApJ*, 685, L13
 Catinella B. et al., 2010, *MNRAS*, 403, 683
 Cayatte V., van Gorkom J. H., Balkowski C., Kotanyi C., 1990, *AJ*, 100, 604
 Chabrier G., 2003, *PASP*, 115, 763
 Cortese L., Hughes T. M., 2009, *MNRAS*, 400, 1225
 Cortese L. et al., 2008a, *MNRAS*, 383, 1519
 Cortese L., Gavazzi G., Boselli A., 2008b, *MNRAS*, 390, 1282
 Fabello S., Catinella B., Giovanelli R., Kauffmann G., Haynes M. P., Heckman T. M., Schiminovich D., 2011, *MNRAS*, 411, 993
 Gallazzi A., Brinchmann J., Charlot S., White S. D. M., 2008, *MNRAS*, 383, 1439
 Gavazzi G., Pierini D., Boselli A., 1996, *A&A*, 312, 397
 Gavazzi G., Boselli A., Scodreggio M., Pierini D., Belsole E., 1999, *MNRAS*, 304, 595
 Gavazzi G., Bonfanti C., Sanvito G., Boselli A., Scodreggio M., 2002, *ApJ*, 576, 135

- Gavazzi G., Boselli A., Donati A., Franzetti P., Scodreggio M., 2003, *A&A*, 400, 451
- Gavazzi G., Boselli A., Cortese L., Arosio I., Gallazzi A., Pedotti P., Carrasco L., 2006, *A&A*, 446, 839
- Gavazzi G., Fumagalli M., Cucciati O., Boselli A., 2010, *A&A*, 517, 73
- Gil de Paz A. et al., 2007, *ApJS*, 173, 185
- Giovanelli R., Haynes M. P., 1985, *ApJ*, 292, 404
- Giovanelli R. et al., 2005, *AJ*, 130, 2598
- Giovanelli R. et al., 2007, *AJ*, 133, 2569
- Gómez P. L. et al., 2003, *ApJ*, 584, 210
- Gunn J. E., Gott J. R. I., 1972, *ApJ*, 176, 1
- Haines C. P., Gargiulo A., Merluzzi P., 2008, *MNRAS*, 385, 1201
- Haynes M. P., Giovanelli R., 1984, *AJ*, 89, 758
- Hughes T. M., Cortese L., 2009, *MNRAS*, 396, L41
- Kannappan S. J., 2004, *ApJ*, 611, L89
- Kauffmann G. et al., 2003, *MNRAS*, 341, 54
- Kent B. R. et al., 2008, *AJ*, 136, 713
- Kroupa P., Tout C. A., Gilmore G., 1993, *MNRAS*, 262, 545
- Larson R. B., Tinsley B. M., Caldwell C. N., 1980, *ApJ*, 237, 692
- McGaugh S. S., de Blok W. J. G., 1997, *ApJ*, 481, 689
- Martin D. C. et al., 2005, *ApJ*, 619, L1
- Morrissey P. et al., 2007, *ApJS*, 173, 682
- Roberts M. S., 1963, *ARA&A*, 1, 149
- Roberts M. S., Haynes M. P., 1994, *ARA&A*, 32, 115
- Saintonge A. et al., 2011, *MNRAS*, in press (arXiv:1103.1642)
- Schiminovich D. et al., 2007, *ApJS*, 173, 315
- Schlegel D. J., Finkbeiner D. P., Davis M., 1998, *ApJ*, 500, 525
- Skrutskie M. F. et al., 2006, *AJ*, 131, 1163
- Solanes J. M., Giovanelli R., Haynes M. P., 1996, *ApJ*, 461, 609
- Solanes J. M., Manrique A., García-Gómez C., González-Casado G., Giovanelli R., Haynes M. P., 2001, *ApJ*, 548, 97
- Springob C. M., Haynes M. P., Giovanelli R., 2005, *ApJ*, 621, 215
- Verheijen M., van Gorkom J. H., Szomoru A., Dwarakanath K. S., Poggianti B. M., Schiminovich D., 2007, *ApJ*, 668, L9
- Vollmer B., Cayatte V., Balkowski C., Duschl W. J., 2001, *ApJ*, 561, 708
- Weinmann S. M., van den Bosch F. C., Pasquali A., 2011, in *Environment and the Formation of Galaxies: 30 Years Later*, preprint (arXiv:1101.3244)
- Wyder T. K. et al., 2007, *ApJS*, 173, 293
- Zhang W., Li C., Kauffmann G., Zou H., Catinella B., Shen S., Guo Q., Chang R., 2009, *MNRAS*, 397, 1243
- Zibetti S., Charlot S., Rix H.-W., 2009, *MNRAS*, 400, 1181

This paper has been typeset from a $\text{\TeX}/\text{\LaTeX}$ file prepared by the author.